JOURNAL OF BACTERIOLOGY, Dec. 2006, p. 8430–8440 Vol. 188, No. 24
0021-9193/06/$08.00+0 doi:10.1128/JB.01085-06

N-Acetylanthranilate Amidase from *Arthrobacter nitroguajacolicus* Rü61a, an α/β-Hydrolase-Fold Protein Active towards Aryl-Acylamides and -Esters, and Properties of Its Cysteine-Deficient Variant▽†

Stephan Kolkenbrock,[1] Katja Parschat,[1] Bernd Beermann,[2] Hans-Jürgen Hinz,[2] and Susanne Fetzner[1]*

Institut für Molekulare Mikrobiologie und Biotechnologie,[1] and Institut für Physikalische Chemie,[2] Westfälische Wilhelms-Universität Münster, D-48149 Münster, Germany

Received 22 July 2006/Accepted 1 October 2006

***N*-acetylanthranilate amidase (Amq), a 32.8-kDa monomeric amide hydrolase, is involved in quinaldine degradation by *Arthrobacter nitroguajacolicus* Rü61a. Sequence analysis and secondary structure predictions indicated that Amq is related to carboxylesterases and belongs to the α/β-hydrolase-fold superfamily of enzymes; inactivation of (His_6-tagged) Amq by phenylmethanesulfonyl fluoride and diethyl pyrocarbonate and replacement of conserved residues suggested a catalytic triad consisting of S155, E235, and H266. Amq is most active towards aryl-acetylamides and aryl-acetylesters. Remarkably, its preference for ring-substituted analogues was different for amides and esters. Among the esters tested, phenylacetate was hydrolyzed with highest catalytic efficiency (k_{cat}/K_m = 208 mM^{-1} s^{-1}), while among the aryl-acetylamides, *o*-carboxy- or *o*-nitro-substituted analogues were preferred over *p*-substituted or unsubstituted compounds. Hydrolysis by His_6Amq of primary amides, lactams, *N*-acetylated amino acids, azocoll, tributyrin, and the acylanilide and urethane pesticides propachlor, propham, carbaryl, and isocarb was not observed; propanil was hydrolyzed with 1% *N*-acetylanthranilate amidase activity. The catalytic properties of the cysteine-deficient variant His_6AmqC22A/C63A markedly differed from those of His_6Amq. The replacements effected some changes in K_ms of the enzyme and increased k_{cat}s for most aryl-acetylesters and some aryl-acetylamides by factors of about three to eight while decreasing k_{cat} for the formyl analogue *N*-formylanthranilate by several orders of magnitude. Circular dichroism studies indicated that the cysteine-to-alanine replacements resulted in significant change of the overall fold, especially an increase in α-helicity of the cysteine-deficient protein. The conformational changes may also affect the active site and may account for the observed changes in kinetic properties.**

The soil bacterium *Arthrobacter nitroguajacolicus* Rü61a (formerly assigned to the species *A. ilicis*) is able to utilize quinaldine (2-methylquinoline) as the sole source of carbon and energy (34, 49; for a review, see reference 19). Quinaldine degradation (Fig. 1) starts with a hydroxylation in position 4 to form 1*H*-4-oxoquinaldine, catalyzed by the molybdenum enzyme quinaldine 4-oxidase (52). A monooxygenase-catalyzed hydroxylation at C-3 subsequently produces 1*H*-3-hydroxy-4-oxoquinaldine, which undergoes an unusual 2,4-dioxygenolytic ring cleavage reaction, yielding carbon monoxide and *N*-acetylanthranilate (20, 21). Anthranilate was identified as a further intermediate; its degradation is assumed to proceed via catechol and the well-known *ortho* cleavage pathway (34). The genes coding for the enzymes involved in quinaldine conversion to anthranilate are clustered on the linear conjugative plasmid pAL1 (49). The open reading frame ("ORF4") located downstream of the gene encoding 1*H*-3-hydroxy-4-oxoquinaldine 2,4-dioxygenase was the only putative hydrolase gene on a DNA fragment that conferred to *Pseudomonas putida* KT2440 the ability to convert quinaldine to anthranilate and thus was supposed to encode *N*-acetylanthranilate amide hydrolase (52).

According to function, *N*-acetylanthranilate amidase belongs to the aryl-acylamidases (EC 3.5.1.13), which catalyze the hydrolysis of *N*-acyl primary aromatic amines (anilides) to form an aniline and a carboxylic acid. Aryl-acylamidases have been detected in animals, plants, and microorganisms. In several vertebrate systems, aryl-acylamidase activity has been shown to be an intrinsic property of acetylcholinesterase (EC 3.1.1.7) and butyrylcholinesterase (EC 3.1.1.8). Cholinesterases contain a catalytic triad (Ser-Glu-His) and belong to the α/β-hydrolase-fold family of enzymes (47, 66). The biological function of this additional reactivity of cholinesterases is not known; however, it has been discussed in several studies that it may be important in embryogenesis and early development of the nervous system and in pathological processes such as formation of neuritic plaques in Alzheimer's disease (5, 12, 14). Cholinesterases are thought to use the same active site, i.e., the same acyl binding pocket and the catalytic triad, for esterase and aryl-acylamidase activity (14).

In plants, aryl-acylamidases are key enzymes in detoxification of acylanilide herbicides (22, 36). The enzyme from rice is susceptible to inhibition by the organophosphates parathion and paraoxon (43), which are potent acetylcholinesterase inhibitors, suggesting an active-site serine residue. However, the

* Corresponding author. Mailing address: Institut für Molekulare Mikrobiologie und Biotechnologie, Westfälische Wilhelms-Universität Münster, Corrensstraβe 3, D-48149 Münster, Germany. Phone: 49 (0)251 83 39824. Fax: 49 (0)251 83 38388. E-mail: fetzner@uni-muenster.de.

† Supplemental material for this article may be found at http://jb.asm.org/.

▽ Published ahead of print on 13 October 2006.

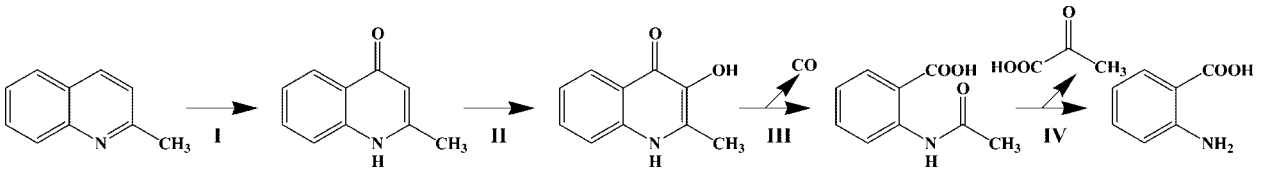

FIG. 1. Conversion of quinaldine (2-methylquinoline) to anthranilic acid by *A. nitroguajacolicus* Rü61a (19, 34). I, quinaldine 4-oxidase; II, 1*H*-4-oxoquinaldine-3-monooxygenase; III, 1*H*-3-hydroxy-4-oxoquinaldine 2,4-dioxygenase; IV, *N*-acetylanthranilate amidase (Amq). For details, see the text.

amino acid (aa) sequence of aryl-acylamidase from *Oryza* spp. has not been identified yet. The enzyme from tulip was reported to lack significant sequence similarity to protein sequences available in databases (22).

Bacterial strains with the ability to degrade acylanilide or phenylcarbamate herbicides have been used as main sources for the isolation of prokaryotic aryl-acylamidases. Biochemical data have been published on enzymes from *Pseudomonas striata* (37), *Bacillus sphaericus* ATCC 12123 (18), *P. acidovorans* AE1 (6, 30), *P. fluorescens* ATCC 39004 (26), *Rhodococcus erythropolis* NCIB 12273 (68), *P. pickettii* (31), and *Nocardia globerula* IFO 13510 (70). Recently, a urethane hydrolase was isolated from *Rhodococcus equi* TB-60, which besides catalyzing cleavage of urethane bonds to release amines effectively hydrolyzes *p*-nitrophenylacetate and acetanilides (3). Apart from the N-terminal sequence of the *N. globerula* protein (Swissprot accession number P80008) and a partial sequence from the active site of *P. acidovorans* aryl-acylamidase (30), sequence information on these bacterial aryl-acylamidases is not available, and therefore their affiliation to protein families is not known. Note that phenylcarbamate hydrolase from *Arthrobacter oxydans* P52, which has only minor amidase activity towards the acylanilide herbicide propanil, shows significant similarity to eukaryotic cholinesterases and carboxylesterases (55).

Here we report on the heterologous expression in *E. coli* of the gene encoding *N*-acetylanthranilate amidase from *A. nitroguajacolicus* Rü61a and some biochemical properties of the enzyme (designated Amq, for amidase involved in quinaldine degradation). Amq is most active towards aryl-acetylamides and -esters; however, its preference for ring-substituted analogues is different for amides and esters. The cysteine-deficient protein His_6AmqC22A/C63A has improved catalytic properties, and circular dichroism (CD) studies indicated that it shows significant changes in its overall fold.

MATERIALS AND METHODS

Bacterial strains, media, and growth conditions. The strains and plasmids used in this study are listed in Table 1. For the isolation of genomic DNA, *A. nitroguajacolicus* Rü61a was grown in mineral salts medium with 8 mM sodium benzoate as the source of carbon and energy at 30°C (52). The same mineral salts medium with 2 mM propanil, and with 2 mM propanil and 2 mM 1*H*-4-oxoquinaldine, was used to assess utilization and cometabolic conversion of propanil. *E. coli* strains were grown in lysogeny broth (62) at 37°C. *E. coli* DH5α (25) harboring pWFAAM and derivatives and *E. coli* M15(pREP4)(pWFAAM) strains producing His_6Amq or His_6Amq protein variants were grown in the presence of ampicillin (100 μg/ml) and ampicillin (100 μg/ml) plus kanamycin (25 μg/ml), respectively. Expression of *amq* was induced by addition of 0.1 mM isopropyl-β-D-thiogalactopyranoside (IPTG) at an optical density at 600 nm of 0.9 to 1.0. Cells were harvested after 3 h of induction at an optical density at 600 nm of about 3.5 by centrifugation at 10,000 × *g* and 4°C for 10 min. The yield of wet biomass of *E. coli* M15(pREP4)(pWFAAM) from a 5-liter bioreactor was about 20 g.

DNA isolation and gene cloning. Total DNA of *A. nitroguajacolicus* Rü61a was isolated according to Rainey et al. (57). Plasmid DNA was isolated with the E.Z.N.A. Plasmid Miniprep kit (peqlab, Erlangen, Germany). Gel extraction of DNA fragments from agarose gels was performed with the Perfectprep gel cleanup kit (Eppendorf, Hamburg, Germany). For cloning purposes, DNA fragments were purified with the High Pure PCR Product Purification kit (Roche, Grenzach-Wyhlen, Germany). Standard protocols were used for agarose gel electrophoresis, restriction digestion, and DNA ligation (63). The *amq* gene (accession no. AJ537472; nucleotides 13840 to 14721) was amplified by PCR with *Pfu* polymerase (Promega, Mannheim, Germany) using total DNA of *A. nitroguajacolicus* Rü61a as template and the primers 5′-GCGGTACCGGGGTGCGAGGGGTTCACCAGAT-3′ (forward) and 5′-ACGACAGGACGGGAGGACACCGCCACGAGG-3′ (reverse). The PCR product was ligated into the StuI/KpnI restriction sites of pQE-30 Xa (QIAGEN, Hilden, Germany), generating pWFAAM. Correct insertion was verified by sequencing the insert as well as flanking regions (MWG Biotech, Ebersberg, Germany). Competent cells of *E. coli* DH5α and *E. coli* M15(pREP4) were generated as described by Hanahan (27). For production of recombinant His_6Amq protein or variants thereof, *E. coli*

TABLE 1. Strains and plasmids used in this study

Strain or plasmid	Description	Source or reference
Strain		
A. nitroguajacolicus Rü61a	Soil isolate; source of *amq* gene; wild type; pAL1	16, 49
E. coli DH5α	*supE44* Δ*lacU169* (Φ80*lacZ*ΔM15) *hsdR17 recAI endAI gyrA96 thi-1 relA1* F^-	25
E. coli M15(pREP4)	Nal^s Str^s Rif^s *lac thi ara*$^+$ *gal*$^+$ *mtl* F^- $RecA^+$ *uvr*$^+$ *lon*$^+$ [pREP4 Kan^r]	QIAGEN
Plasmid(s)		
pREP4	Repressor plasmid; 3.7 kb; *lacI*; Km^r	QIAGEN
pQE-30 Xa	*lacO*; His_6; ColE1 replicon; T5 promoter; Amp^r	QIAGEN
pWFAAM	882-bp PCR product encoding *amq* inserted in StuI/KpnI site of pQE-30 Xa	This work
pWFAAM-C22A, pWFAAM-C63A, pWFAAM-C22A/C63A, pWFAAM-S155A, pWFAAM-E235A, pWFAAM-H266A	pWFAAM derivatives, carrying mutations in *amq* for the production of His_6AmqC22A, His_6AmqC63A, His_6AmqC22A/C63A, His_6AmqS155A, His_6AmqE235A, and His_6AmqH266A	This work

M15(pREP4) was transformed with pWFAAM or derivatives isolated from *E. coli* DH5α clones.

Site-directed mutagenesis. Site-directed mutagenesis was performed according to the protocol of the QuikChange site-directed mutagenesis kit (Stratagene, Heidelberg, Germany) using pWFAAM as template, *Pfu* polymerase for amplification, and the mismatch primer pairs listed in the table in the supplemental material. Sequencing of the inserts and flanking regions of all mutant plasmids was performed by MWG Biotech.

Preparation of cell extracts and purification of recombinant His_6Amq proteins. Twenty grams of cells (wet biomass) of *E. coli* M15(pREP4) containing pWFAAM (or derivatives) was suspended in 40 ml 50 mM sodium phosphate buffer containing 10 mM imidazole and 300 mM NaCl (pH 8.0). Crude extract containing soluble proteins was obtained by sonication (sonifier UP200s; Dr. Hilscher GmbH, Stuttgart, Germany) and subsequent centrifugation at 40,000 × *g* and 4°C for 40 min. The supernatant was applied to an Ni-Sepharose High Performance column (GE Healthcare Europe, Munich, Germany; 10-ml bed volume in Bio-Scale MT10 column from Bio-Rad Laboratories, Munich, Germany), equilibrated in 50 mM sodium phosphate buffer containing 10 mM imidazole, 3 mM dithiothreitol (DTT), and 300 mM NaCl (pH 8.0). After washing with the same buffer, His_6Amq was eluted with a linear gradient (30 ml) of 20 to 250 mM imidazole in equilibration buffer. Fractions containing His_6Amq were pooled and washed in 40 mM Britton-Robinson (BR) buffer (58) (pH 7.5; 12.5% [vol/vol] glycerol added) by ultrafiltration (Vivaspin 20; molecular weight cutoff, 10,000; Vivascience, Hannover, Germany). The concentrated protein solution was diluted in 50 mM Tris-HCl buffer (pH 8) and loaded onto an UNOsphere Q column (2-ml bed volume; Bio-Rad) equilibrated in the same buffer. After a washing step, His_6Amq was eluted in a linear gradient (32 ml) from 0 to 300 mM NaCl in 50 mM Tris-HCl buffer (pH 8.0). Fractions containing the enzyme were washed and concentrated in BR buffer (pH 7.5, with 12.5% [vol/vol] glycerol) by ultrafiltration and stored at −20°C. Protein samples for CD spectroscopy were dialyzed for 15 h against 10 mM sodium phosphate buffer, pH 7.5.

For enrichment of His_6AmqS155A, His_6AmqE235A, and His_6AmqH266A, 0.1 mM 4-(2-aminoethyl) benzenesulfonyl fluoride hydrochloride (AEBSF) was added to the cell suspension prior to sonication.

Removal of the His_6 tag. The N-terminal His_6 tag of His_6Amq was removed by treatment with Factor Xa protease (QIAGEN) according to the manufacturer's instructions (The QIA*expressionist*; QIAGEN GmbH, Hilden, Germany). Optimal cleavage without formation of unspecific degradation products was achieved by incubation of 10 μg His_6Amq (0.25 μg/μl) with 0.2 U Factor Xa protease for 2.5 h at room temperature. The His_6 tag and residual His_6Amq was removed by loading the reaction mix on an Ni-nitrilotriacetate Spin Column (QIAGEN) and centrifugation at 8,000 × *g*.

Enzyme assays and kinetics. Stock solutions of potential substrates (50 mM) and their hydrolysis products were prepared in ethanol. Since incubation of His_6Amq (0.11 μM) with up to 5 mM EDTA did not inhibit its activity, the amidase assays were routinely performed with buffer containing 100 μM EDTA to protect the enzyme from divalent heavy-metal cations. In the spectrophotometric standard assay, carried out in BR buffer (40 mM, pH 8) with 100 μM EDTA at 25°C, enzyme-catalyzed formation of anthranilate from *N*-acetylanthranilate (5 mM) was measured at 325 nm (ε_{325} = 2.012 mM^{-1} cm^{-1}). In preliminary tests for His_6Amq-catalyzed conversion of other (aromatic) amides and esters, UV/Vis spectra (250 to 600 nm) were taken at appropriate time intervals of an assay mixture that contained 5 mM of the potential substrate and 0.06 μM of His_6Amq. Quantitative spectrophotometric determinations of products generated by enzyme-catalyzed hydrolysis of aryl-acylamides or -esters were based on the following molar extinction coefficients (in assay buffer): 2-nitroaniline, ε_{420} = 4.438 mM^{-1} cm^{-1}; 2-chloroaniline, ε_{290} = 1.670 mM^{-1} cm^{-1}; 2-bromo-4-methylaniline, ε_{295} = 1.966 mM^{-1} cm^{-1}; aniline, ε_{285} = 1.152 mM^{-1} cm^{-1}; phenol, ε_{270} = 1.068 mM^{-1} cm^{-1}; *p*-nitrophenol, ε_{400} = 14.847 mM^{-1} cm^{-1}; salicylic acid, ε_{298} = 3.162 mM^{-1} cm^{-1}; 3,4-dichloroaniline, ε_{305} = 1.99 mM^{-1} cm^{-1}. One unit was defined as the amount of enzyme that catalyzes the formation of 1 μmol of product in 1 min under the conditions described. For the determination of kinetic constants K_m and k_{cat}, concentrations of 1 to 5 mM were used for all substrates except phenylacetate and *p*-nitrophenylbutyrate, which were assayed at 0.05 to 2 mM and 0.05 to 1.5 mM, respectively. Apparent kinetic constants were deduced from Hanes plots (28). Assays were done at least in triplicate.

The activity of His_6Amq was assessed in the presence of some organic solvents. Their partition coefficient log *P* was calculated by the java applet Marvin with default values (ChemAxon Ltd.; http://intro.bio.umb.edu/111-112/OLLM/111F98/newclogp.html).

Hydrolysis of *N*-acetylated amino acids (5 mM) by His_6Amq (0.06 μM) was measured as release of acetic acid in the phenol red assay described by Holloway et al. (32). This assay was sensitive enough to detect the release of 0.4 mM acid from 5 mM phenylacetate. Hydrolysis of primary amides (5 mM) by His_6Amq (0.06 μM) was examined by determining release of ammonia (69).

To assess the potential of His_6Amq for hydrolysis of the natural polyamide cyanophycin, a suspension of cyanophycin was treated with 6 μM enzyme in BR buffer and degradation products carrying amino groups were determined by high-performance liquid chromatography (HPLC) and fluorescence detection after precolumn derivatization with *o*-phthaldialdehyde, as described in Aboulmagd et al. (1). Proteolytic activity of His_6Amq was tested by incubation of the protein (0.6 μM and 1.2 μM) with a suspension of azocoll (1.5 mg) for 30 min at 30°C and subsequent spectrophotometric detection of soluble dye-coupled peptides in the supernatant at 520 nm (13).

To test for triacylglycerol hydrolase activity, 10 μl of His_6Amq (67 μM) was applied on a tributyrin agarose plate (1% [wt/vol] agarose, 1% [vol/vol] Tween 80, 0.25% [vol/vol] tributyrin in BR buffer, pH 8) and incubated for 24 h at 25°C. Application of *o*-nitroacetanilide (5 mM in BR buffer, pH 8) to the tributyrin plate after the incubation period resulted in formation of yellow 2-nitroaniline by His_6Amq, indicating that the enzyme was still functional. As a positive control, 2.5 μM of an esterase (accession no. AJ537472; ORF7) active towards tributyrin was applied to the same plate, which formed a spot of clearance in the opaque layer.

Protein analysis. Protein concentrations were estimated by the Bradford method as modified by Zor and Selinger (72). For CD spectroscopy, concentrations of electrophoretically pure His_6Amq and His_6AmqC22A/C63A were deduced from the theoretical molar extinction coefficients at 280 nm, calculated according to Pace et al. (51): ε_{280} = 1.278 liter g^{-1} cm^{-1} for His_6Amq and ε_{280} = 1.277 liter g^{-1} cm^{-1} for the cysteine-deficient protein. Denaturing sodium dodecyl sulfate-polyacrylamide gel electrophoresis (SDS-PAGE) was performed as described by Laemmli (39), using an overall acrylamide concentration of 10.8% and a cross-linker concentration of 2.6% in the separating gels. For nondenaturing (native) PAGE, the Laemmli method was used, omitting SDS from the buffers. Polyacrylamide gels were stained with Coomassie blue R-250 (0.1% [wt/wt] Coomassie blue R-250, 50% [wt/wt] trichloroacetic acid in H_2O) and destained in an aqueous solution of 30% (vol/vol) methanol and 10% (vol/vol) acetic acid. Transfer of proteins (67) from gels to polyvinylidene fluoride membranes (Carl Roth, Karlsruhe, Germany) was performed according to the protocol of QIAGEN (QIA*express*). Immunodetection of His_6-tagged proteins on blots was performed using primary antibodies [anti-$(His)_5$ mouse immunoglobulin G1; QIAGEN], secondary antibodies (horseradish peroxidase-conjugated sheep anti-mouse immunoglobulin G; Chemicon International), and *p*-nitrotetrazolium blue and 5-bromo-4-chloro-3-indolyl phosphate for colorimetric detection (QIA*express* protocol; QIAGEN).

Gel filtration of His_6Amq for determination of its native molecular mass was performed on a Bioprep SE-1000/17 column (Bio-Rad Laboratories) in 50 mM sodium phosphate buffer containing 150 mM NaCl (pH 7.5). A gel filtration standard marker from Bio-Rad was used for calibration of the column.

Shelf stability of His_6Amq and pH and temperature optima of activity. Stability of His_6Amq was measured in 20 mM Tris-HCl, 50 mM sodium phosphate, and 40 mM BR buffer in a pH range of 6.0 to 8.0 at temperatures of −20°C, 4°C, and 25°C. Residual enzyme activity was determined in the standard enzyme assay with aliquots of 0.06 μM His_6Amq. The activity of His_6Amq at different pHs was tested in the same buffers (Tris-HCl, pH 7 to 9; sodium phosphate, pH 6.2 to 8.2; BR, pH 4.5 to 11). Temperature dependence of His_6Amq activity was determined in the buffer of the standard assay.

Chemical modification of amino acid residues and potential effectors of His_6Amq. Since conserved serine and histidine residues of Amq were hypothesized to be catalytically relevant, the influence of phenylmethylsulfonyl fluoride (PMSF) and diethyl pyrocarbonate (DEPC) on enzyme activity was measured in concentrations of 0 to 70 μM and 0 to 2 μM, respectively. Additionally, the effect of $HgCl_2$ (0 to 0.2 μM) was tested. Samples of His_6Amq (6 μM) in 40 mM BR buffer (without EDTA) were preincubated with potential inhibitor for 10 min at room temperature, and residual activity towards *N*-acetylanthranilate was measured spectrophotometrically in the same buffer using aliquots of 0.06 μM His_6Amq.

The influence of EDTA (5 μM to 30 mM) and DTT (1 to 50 mM) on His_6Amq activity was analyzed in the standard enzyme assay, omitting EDTA from the BR buffer. To assess the effect of divalent metal cations, *N*-acetylanthranilate amidase activity was determined after incubation of 0.11 μM His_6Amq with metal salts (10 and 100 μM) in BR buffer (40 mM, pH 8, without EDTA) for 5 min.

CD spectroscopy. CD spectra were recorded using a Jobin-Yvon (Paris, France) Spectropolarimeter model CD6 equipped with a peltier-thermostated cell holder, which was constructed by the machine shop of the Institut für Physikalische Chemie of the University of Münster. Temperature was controlled

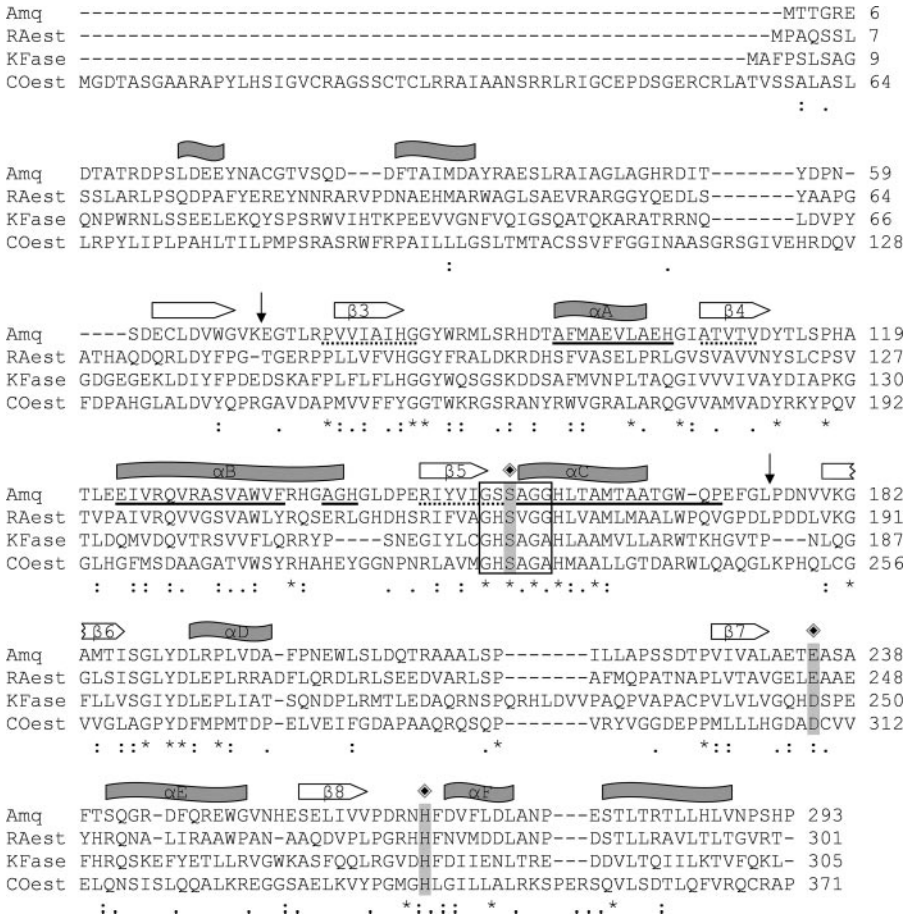

FIG. 2. Multiple alignment of Amq (EMBL accession no. CAD61042) and related proteins, performed with the Clustal W algorithm (2). COest, carboxylesterase from *Xanthomonas axonopodis* pv. *citri* strain 306 (15) (AAM37245); KFase, kynurenine formamidase from *Mus musculus* (50) (AAM44406); RAest, hypothetical esterase from *Ralstonia eutropha* JMP134 (46) (AAZ64529). Residues conserved throughout are marked with an asterisk, while residues marked with a colon and dot indicate conserved and semiconserved substitutions, respectively. Residues of the putative catalytic triad are highlighted in gray and are marked with a diamond. The conserved motif (G-X-S-X-G-G/A) surrounding the catalytic nucleophile of the α/β hydrolase-fold enzymes is enclosed in a box. α-Helical regions and β-strands predicted for Amq by the program PredictProtein (61) are marked with wavy shaded boxes and large white arrows, respectively. Amino acid sequences of Amq that are underlined with continuous and broken lines indicate α-helices and β-strands, respectively, as shown in the three-dimensional model of the core region of Amq (aa 71 to 175, framed by vertical arrows), calculated with ProModII 3.70 (64).

to a precision of ±0.1 K. Quartz cells of 0.01-cm optical path length were used with protein concentrations between 0.8 and 2.0 mg/ml; a path length of 0.1 cm was employed with concentrations between 0.1 and 0.8 mg/ml. The results were expressed as mean residue ellipticity (MRE): $[\Theta]_{MRE} = (MRW\ \theta_{obs})/(cd)$, where θ_{obs} is the observed ellipticity at the respective wavelength, MRW is the mean residue weight of the protein (108,852 g/mol for His_6Amq and 108,647 g/mol for His_6AmqC22A/C63A), d is the optical path length of the cell, and c is the specific concentration (in milligrams/milliliter) of the samples. Deconvolution of CD spectra was done using the programs K2D of Andrade et al. (8) and CDNN of Böhm et al. (11).

RESULTS

Amino acid sequence analysis. BLASTP analysis (7) of the Amq protein (293 amino acids [aa], calculated molecular mass of 32.8 kDa) revealed significant sequence similarity to putative esterases from *Bordetella* spp. (CAE40678; 39% aa identity, 47.7% aa similarity) and *Ralstonia eutropha* JMP134 (46) (AAZ64529; 32.7% aa identity, 41.6% aa similarity) and a hypothetical protein from *Pseudomonas* sp. strain CA10 (BAB32459.1; 39.9% identity). Other related proteins include, for example, carboxylesterase from *Xanthomonas axonopodis* pv. *citri* 306 (15) (AAM37245; 26% aa identity) and kynurenine formamidase from *Mus musculus* (50) (AAM62284; 28% aa identity).

Secondary structure prediction (60, 61) for Amq (Fig. 2) suggested a pattern of β-strands and α-helices which matches that of the "canonical" α/β-hydrolase fold (29, 45, 47). Using core regions of bacterial heroin esterase (Her) (1LZL_A, 1LZK_A) and esterase Est2 from *Alicyclobacillus acidocaldarius* (1U4N_A, 1EVQ_A, 1QZ3_A) as templates, which show a degree of sequence identity to the corresponding region of Amq (aa 71 to 175) of 40.15% (Her) and 35.85% (Est2), the program ProModII (64) calculated a three-dimensional model for this region of Amq. Validation analysis with WHATCHECK (33) revealed an exceedingly good Ramachandran plot appearance Z-score of −0.175. The three-dimensional model comprises the elements β3, αA, β4, αB-αB′, β5, and αC (Fig. 2) and thus supports the secondary structure prediction for this central segment.

The catalytic residues of the α/β-hydrolases constitute a highly conserved catalytic triad consisting of a nucleophile, an acidic residue, and an absolutely conserved histidine. The nucleophile is located at the top of a sharp turn, called the nucleophile elbow, which is characterized by the consensus sequence Sm-X-Nu-X-Sm-Sm (Sm, small residue; X, any residue; and Nu, nucleophile) (47); this motif is clearly conserved in Amq (^{153}GSSAGG^{158}). The signature GxSAG, found in acetylcholinesterase and butyrylcholinesterase, is thought to be typical for many carboxylesterases (54). The presumed nucleophile of Amq (S155) is predicted to be situated between β5 and αC (Fig. 2), and the model calculated with ProModII positions its side chain at the apex of a sharp turn, consistent with the canonical fold (29, 45, 47). If E235 and H266 of Amq represent the other triad residues (Fig. 2), Amq shares with acetylcholine esterases and *p*-nitrobenzyl esterase of *Bacillus subtilis* (71) the use of glutamate instead of the more frequent aspartate as the active-site carboxylate of serine hydrolases. The topological positions of E235 and H266 after predicted strand β7 and between β8 and helix αF, respectively, match the criteria of the α/β-hydrolase fold (29, 45, 47).

The oxyanion hole of most α/β-hydrolases comprises two residues which donate their backbone amide protons to stabilize the negative charge of the transition state. One residue is located adjacent to the nucleophile (Nu + 1), whereas the other is situated in a turn between β3 and αA in the canonical fold (10, 47). Amq, like many α/β-hydrolases, contains an HGX motif (^{82}HGG^{84}) in this region (10, 17, 54) and thus belongs to the "GX-type hydrolases," with X presumed to be the second oxyanion hole residue; the "GX class" of hydrolases comprises many esterases and lipases. In contrast, acetylcholine esterases and other carboxylesterases as well as members of the hormone-sensitive lipase/esterase family belong to the "GGGX class"; in *Torpedo californica* acetylcholinesterase, the peptidic NH groups of G118 and G119 together with the backbone NH group of the Nu + 1 residue A201 actually form a tridentate oxyanion hole (48). The GGGX motif forms a flexible "glycine loop" which is involved in determining the active-site architecture and thus its reactivity towards substrates and inhibitors (48). However, in the absence of structural data, it is unclear whether the ^{82}HGGY^{85} motif of Amq might also represent a short glycine loop.

A search for conserved domains (41) in Amq revealed significant similarity with part of the esterase/lipase domain cd00312 (aa 58 to 158 of Amq, 23.3% aligned). This domain family includes large enzymes with aryl-acylamidase/-esterase activity, namely, acetylcholinesterases, *p*-nitrobenzyl hydrolase (71), and phenylcarbamate hydrolase from *Arthrobacter oxydans* P52 (55). Amq indeed shows similarity to acetylcholinesterase (e.g., from *Torpedo californica*), especially in the region surrounding the nucleophile elbow; however, acetylcholinesterase has a large insertion in the region between β6 and αD, and its C-terminal region (aa 434 to 586 of P04058) does not align with Amq. A segment comprising aa 75 to 202 of Amq is similar to part of a conserved domain of the Aes (acetylesterase) family (COG0657.1; esterase/lipase; 40.1% aligned), and parts of the related consensus sequences of pfam00135 (carboxylesterases) and COG2272 (type B carboxylesterase) also align with a region of Amq (aa 58 to 163 and aa 35 to 168, respectively). Since the physiological role of Amq in strain Rü61a clearly is that of an amidase involved in the quinaldine degradation pathway, catalyzing the hydrolysis of *N*-acetylanthranilate to anthranilate and acetate, its marked similarity with esterases is remarkable and prompted us to study its substrate specificity.

TABLE 2. Purification of His_6Amq from *E. coli* M15(pREP4)(pWFAAM) (20 g wet biomass)[a]

Purification step	Total protein (mg)	Total activity (U)	Sp act (U/mg)	Yield (%)	Purification (*x*-fold)
Crude extract	1,094	1,323	1.2	100	1
Ni sepharose	6.6	432	65	32.7	54
AEX	2.6	234	89	17.7	74

[a] AEX, anion exchange chromatography. Catalytic activity was measured with the physiological substrate *N*-acetylanthranilate.

Purification of His_6Amq and effect of the His_6 tag on amidase activity. Highest yields of His_6Amq from *E. coli* M15(pREP4)(pWFAAM) were obtained from cells grown at 37°C and harvested after 3 h of induction with IPTG. From the soluble fraction of cell extract, His_6Amq was purified 74-fold in a two-step procedure to electrophoretic homogeneity (Table 2; Fig. 3A and B). Detection in Western blots of His_6-tagged proteins showed only small amounts of protein in the insoluble fraction of cell extract (redissolved in 10% SDS). A molecular mass of 34 kDa was deduced from SDS-PAGE, which matches the calculated mass of the tagged protein (313 aa) of 34,070 Da. Gel filtration indicated a molecular mass of 32.2 kDa, suggesting that His_6Amq is a monomeric protein in its native state.

Removal of the His_6 tag by treatment with Factor Xa protease and trapping of the tag and of residual uncleaved His_6Amq yielded electrophoretically pure Amq protein. His_6Amq and Amq showed the same K_ms for *N*-acetylanthranilate, but the apparent k_{cat} of Amq was about 65% of that of His_6Amq (see Table 5), resulting in a catalytic efficiency k_{cat}/K_m of 31 mM^{-1} s^{-1} for His_6Amq and 20 mM^{-1} s^{-1} for Amq. Very similar results were obtained for K_m and k_{cat} of Amq and His_6Amq for the ester acetylsalicylic acid. The apparent K_m was hardly affected, whereas k_{cat} of Amq was 58% of that of His_6Amq (see also Table 5). Such decrease in apparent k_{cat} of Amq may well be caused by the conditions during Factor Xa protease treatment of His_6Amq, which involves protease digestion for 2.5 h in 20 mM Tris-HCl (pH 6.5) at 23°C. Incubation of His_6Amq in this buffer for the same time period resulted in significant loss of specific activity.

Shelf stability and conditions for activity of His_6Amq. Among the buffers, pHs, and temperatures tested, stability of His_6Amq was highest in BR buffer (pH 7.5) at −20°C. Storage for 160 h in this buffer at −20°C retained 91% of activity, whereas losses of 58% and 55% of activity were observed when the enzyme was kept frozen for the same time in 50 mM Tris-HCl (pH 7.5) and 50 mM sodium phosphate buffer (pH 7.5), respectively. Glycerol (12.5%) was added to the storage buffer for long-term freezing; a negative impact of glycerol on enzyme stability and activity was not observed. Highest activity of His_6Amq was measured in BR buffer at pH 8.0 and at a temperature of 30°C (Fig. 4). In Tris buffer (20 mM Tris/HCl, pH 8.0) in the absence of reducing agents, purified His_6Amq

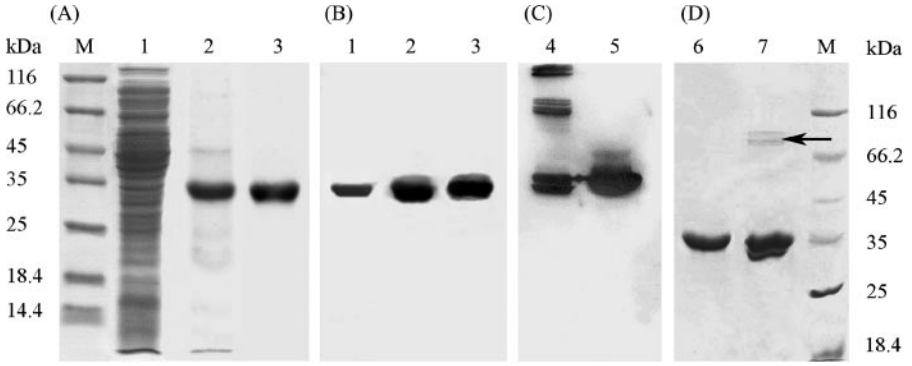

FIG. 3. Purification of His_6Amq from *E. coli* M15(pREP4)(pWFAAM) and electrophoretic properties of His_6Amq and His_6AmqC22A/C63A. (A) SDS-PAGE and (B) corresponding Western blot of proteins after each purification step. Lane M, protein standard; lane 1, crude extract from *E. coli* M15(pREP4)(pWFAAM) (30 μg protein); lane 2, His_6Amq after Ni^{2+} chelate affinity chromatography (5 μg protein); lane 3, His_6Amq after anion exchange chromatography (5 μg protein). (C) Western blot of His_6Amq after Ni^{2+} chelate affinity chromatography in the absence (lane 4) and presence (lane 5) of DTT (20 μg protein in each lane). (D) SDS-PAGE of His_6AmqC22A/C63A (lane 6, 8 μg protein) and His_6Amq (lane 7, 10 μg protein) in the absence of DTT; the arrow indicates dimers of His_6Amq.

existed in two monomeric forms with different electrophoretic mobilities, and it formed dimers (Fig. 3C and D). When preparations after Ni^{2+} affinity chromatography were concentrated in Tris buffer in the absence of DTT, even multimers were observed (Fig. 3C, lane 4). Treatment with DTT eliminated both the second monomeric form and the multimers (Fig. 3C, lane 5), suggesting that they resulted from oxidative formation of intra- and intermolecular disulfide bonds, respectively. Notably, formation of additional protein forms due to disulfide bond formation and increase in activity by addition of DTT were not observed for His_6Amq stored in the BR buffer. The Amq protein contains only two cysteine residues, which were both replaced by alanine. In contrast to His_6Amq, the His_6AmqC22A/C63A protein was stable as a single monomeric form (Fig. 3D, lane 6).

Amidase activity was significantly influenced by the presence of organic solvents. For instance, relative residual activities of 4% and 46% were observed in the presence of 5% (vol/vol) trichloromethane (log $P = 1.61$) and 5% acetonitrile (log $P = -0.33$), respectively. Dimethyl sulfoxide (log $P = -1.43$) and dimethyl formamide (log $P = -0.64$) had a less drastic effect (residual activities of 90% and 72%, respectively, at 5% solvent concentration). A clear correlation between log P values and activity of His_6Amq was, however, not obvious (38).

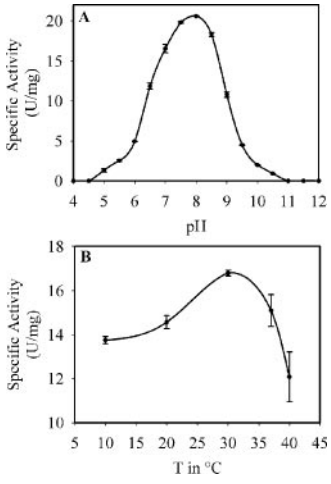

FIG. 4. Effects of pH (A) and temperature (B) on His_6Amq activity towards the physiological substrate *N*-acetylanthranilate.

Putative catalytic triad residues of Amq. To assess the hypothesis of a putative catalytic triad, PMSF and DEPC were used to modify serine and histidine, respectively, and the conserved residues S155, E235, and H266 were replaced by site-directed mutagenesis. Both PMSF and DEPC at micromolar concentrations decreased the apparent V_{max} of His_6Amq without changing its apparent K_m, suggesting partial irreversible inactivation of the enzyme (data not shown). It is interesting to note that the serine hydrolase inhibitor AEBSF in concentrations up to 0.5 mM did not affect the activity of His_6Amq.

Replacement of the potential triad residues (Fig. 2) by alanine resulted in drastically decreased yields of protein in cell extracts. Addition of the protease inhibitor AEBSF to the cell suspension prior to sonication was necessary to prevent loss of the proteins. SDS-PAGE and Western blot analysis of both soluble and insoluble fractions of the cell extracts after resuspension in 10% SDS indicated that the respective recombinant *E. coli* cells contained only small amounts of His_6AmqH266A, His_6AmqE235A, or His_6AmqS155A protein in the soluble fractions. The immunodetection of His_6-tagged proteins on Western blots failed to show any signal for the proteins of the insoluble fractions. We thus assume that loss of these protein variants is due to their high susceptibility to proteolytic degradation rather than formation of inclusion bodies. Some enrichment by Ni^{2+} affinity chromatography was possible, but subsequent anion exchange chromatography led to complete loss of the proteins. In standard assays containing up to 0.17 mg of protein prepared by metal chelate chromatography, *N*-acetylanthranilate amidase activity of the His_6AmqE235A and -S155A preparations was below the detection limit of the spectrophotometric assay (more than 212-fold decrease in activity). Replacement of H266 resulted in major reduction but not abolition of activity. A residual activity of 0.11 U/mg was detected in the preparation of His_6AmqH266A, which contained many contaminating proteins. Such residual activity was unexpected, since substitution of the active-site histidine of α/β-

TABLE 3. Relative catalytic activity of His_6Amq (0.11 μM) after incubation for 5 min in BR buffer (40 mM, pH 8) containing different metal cations

Metal salt	Relative activity as function of metal ion concn of:	
	100 μM	10 μM
$FeCl_2$	127	117
$CaCl_2$	109	116
$NiCl_2$	105	109
$MnCl_2$	100	117
$CoCl_2$	99	102
$MgCl_2$	91	112
$CuSO_4$	80	110
$ZnCl_2$	44	58
$HgCl_2$	35	83
$CdSO_4$	24	87

hydrolases generally resulted in inactive proteins, consistent with the role of this residue as an essential catalytic base (4, 9, 17, 24, 35, 44, 53, 56, 65). However, reports on protein variants of C-C hydrolase MhpC (40) and *Agrobacterium radiobacter* epoxide hydrolase (59) show that the observation of minor residual activity after replacement of the triad's histidine is not unprecedented. Such residual activity may be due to specific base catalysis by solvent OH^- (40).

Role of cysteine residues of Amq. As shown in Table 3, incubation of His_6Amq with an excess of Zn^{2+}, Hg^{2+}, and Cd^{2+} resulted in drastic decreases in *N*-acetylanthranilate amidase activity. These effects were reversible by EDTA. When Amq activity was measured in the presence of micromolar concentrations of $HgCl_2$ (without EDTA), the apparent V_{max} of the enzyme was decreased while its apparent K_m was not affected, suggesting partial inactivation of the enzyme. Since Cd^{2+} and Hg^{2+} preferably bind to sulfhydryl groups, this observation might suggest that cysteine is involved in catalysis. However, since sequence analysis of Amq predicted an α/β-hydrolase-fold protein with a canonical catalytic triad, the potential role of cysteine in substrate turnover was enigmatic. Actually, inhibition of His_6AmqC22A/C63A (0.025 to 0.05 μM) by 10 and 100 μM Hg^{2+}, Cd^{2+}, and Zn^{2+} was similar as observed for His_6Amq (data not shown), indicating unspecific inactivation rather than group-specific cysteine modification.

Substrate specificity of Amq. Release of ammonia from the primary amides tested (acetamide, propionamide, acrylamide, benzamide, and nicotinamide) and hydrolysis of urea or thiourea were not observed after incubation of 1 U (*N*-acetylanthranilate amidase activity) of His_6Amq with up to 25 mM of potential substrate for 18 h at 30°C. Ammonia quantification would have been sensitive enough to detect a relative activity of 0.18% of *N*-acetylanthranilate amidase activity. In contrast to acetanilides with an acidic or polar substituent in *ortho* position (see below), conversion of the following anilides was not detected: *o*-aminoacetanilide, *m*-nitroacetanilide, *m*-hydroxyacetanilide (3-acetamidophenol), *p*-nitroacetanilide, and benzanilide. Compounds that also were not hydrolyzed include *N*-phenyl urea, 1,1-carbonyldiimidazol, the benzoate derivatives benzohydroxamate and hippurate, the lactams penicillin G, ampicillin, and ε-caprolactame, the cyclic compounds succinimide, barbiturate, 5-bromouracil, and imidazolidine-2-thione, the polyamide cyanophycin, the chromogenic protein azocoll, and the ester acetylcholine chloride. Hydrolysis of tributyrin was not evident in a qualitative plate assay. Release of acid from *N*-acetylated amino acids (*N*-acetyl-glycine, *N*-acetyl-DL-leucine, *N*-acetyl-DL-glutamate, *N*-acetyl-DL-valine, *N*-acetyl-DL-alanine, *N*-acetyl-DL-proline, *N*-acetyl-DL-tryptophan, *N*-acetyl-DL-serine, *N*-acetyl-DL-phenylalanine, *N*-acetyl-L-cysteine, and *N*-acetyl-DL-methionine) also was not observed.

The activity of Amq towards *N*-acetylanthranilate and other anilides suggested that acylanilide pesticides also might be accepted as substrates. Actually, the herbicide propanil (3′,4′-dichloropropionanilide) was hydrolyzed by His_6Amq with a specific activity of 0.95 U/mg, i.e., about 1% of *N*-acetylanthranilate amidase activity. However, *A. nitroguajacolicus* Rü61a neither grows on nor cometabolically converts propanil. Hydrolysis of propachlor (2′-chloro-*N*-isopropylacetanilide), which carries a tertiary amine, was not detected when up to 0.3 μM of His_6Amq was used in the phenol red assay or in UV/Vis spectral analyses. Hydrolysis of the urethane herbicides propham (isopropyl phenylcarbamate), carbaryl (1-naphthyl-*N*-methylcarbamate), and isoprocarb (2-isopropylphenyl-*N*-methylcarbamate) likewise was not observed.

With the substrates tested, His_6Amq showed typical Michaelis Menten kinetics. Its kinetic parameters for a series of secondary amides and esters are shown in Table 4. Replacement of the acetyl group of the physiological substrate by a formyl moiety (*N*-formylanthranilate) increased the K_m about 10-fold (while increasing k_{cat} by a factor of about 2). The aryl-acetylester *p*-nitrophenylacetate was preferred over the corresponding butyrate ester. Thus, Amq may be described as an aryl-acetylamidase/-esterase. Among the acetanilides, Amq converts derivatives with a polar (*o*-nitroacetanilide, *o*-chloroacetanilide) or acidic (*N*-acetylanthranilate) substituent in *ortho* position with high activity. Lack of activity towards *o*-aminoacetanilide suggests that a basic substituent in *ortho* position prevents conversion. Acetanilide derivatives monosubstituted in *meta* or *para* position (*m*- and *p*-nitroacetanilide) were not hydrolyzed, whereas the disubstituted compound 2′-bromo-4′-methylacetamide was converted, albeit with low efficiency (K_m and k_{cat} of His_6Amq of about 12 mM and 9.5 s^{-1}, respectively). Among the amides listed in Table 4, hydrolysis of the nonsubstituted acetanilide was catalyzed with lowest efficiency, mainly due to a k_{cat} of only 0.8 s^{-1}. Remarkably, the corresponding ester phenylacetate was converted best, with a very low K_m and high k_{cat} and an almost sevenfold-increased catalytic efficiency compared with turnover of the physiological substrate. The notion that Amq prefers different substitution patterns for aryl-acetylamides and aryl-acetylesters is supported by the kinetic parameters observed for *para*-substituted substrates. While *p*-nitroacetanilide was not converted, hydrolysis of *p*-nitrophenylacetate was catalyzed at a high rate (Table 4).

The preferences of the protein variant His_6Amq-C22A/C63A for differently substituted aryl-acylamides and -esters roughly follow those of His_6Amq for most, but not all, substrates tested (Table 4). A drastically decreased k_{cat} of His_6AmqC22A/C63A was observed with *N*-formylanthranilate. Remarkably, the cysteine-deficient protein showed decreased K_m and increased k_{cat} towards phenylacetate and the *ortho*-carboxy-substituted compounds *N*-acetylanthranilate and

TABLE 4. Substrate specificity and apparent kinetics constants of His_6Amq and His_6AmqC22A/C63A[a]

Formula	His_6Amq			His_6AmqC22A/C63A		
	K_m (mM)	k_{cat} (s^{-1})	Catalytic efficiency k_{cat}/K_m (mM^{-1} s^{-1})	K_m (mM)	k_{cat} (s^{-1})	Catalytic efficiency k_{cat}/K_m (mM^{-1} s^{-1})
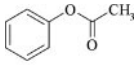 phenylacetate	0.6	125	208	0.3	425	1,417
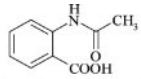 *N*-acetylanthranilic acid	3.2	98	31	1.4	316	226
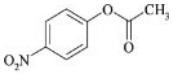 *p*-nitrophenylacetate	3.2	92	29	16.3	494	30
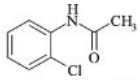 *o*-chloroacetanilide	9.9	103	10	21.2	106	5
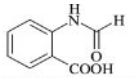 *N*-formylanthranilic acid	31.7	217	7	13.6	0.03	0.002
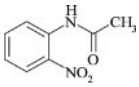 *o*-nitroacetanilide	7.9	53	7	45.6	138	3
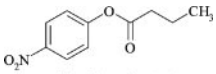 *p*-nitrophenylbutyrate	2.2	10	4.5	2.3	17	7.4
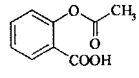 acetylsalicylic acid	15.6	54	3.5	4.5	447	99
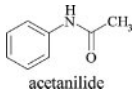 acetanilide	2.8	0.8	0.3	26.2	6.4	0.24

[a] Standard deviations for all apparent K_m s were below ±20% of the value given, except for a K_m of His_6AmqC22A/C63A for *N*-formylanthranilate of 16.3 ± 7 mM. Standard deviations for all k_{cat} s were below ±10%, except k_{cat} of His_6AmqC22A/C63A for *p*-nitrophenylacetate of 494 ± 86 s^{-1} and for *N*-formylanthranilate of 0.03 ± 0.012 s^{-1}.

acetylsalicylate, resulting in pronounced increases in catalytic efficiency compared to that of His_6Amq. Actually, about three- to eightfold increases in turnover numbers of His_6AmqC22A/C63A were observed for all aryl-acetylesters and aryl-acetylamides tested, except *o*-chloroacetanilide. However, the increases in k_{cat} towards *p*-nitrophenylacetate, *o*-nitroacetanilide, and acetanilide were compensated by increases in K_m, resulting in somewhat similar catalytic efficiencies of His_6Amq and His_6AmqC22A/C63A towards these compounds.

During protein purification, the increase in specific activity of His_6AmqC22A/C63A towards the physiological substrate *N*-acetylanthranilate correlated with a similar increase in specific activity towards the ester analogue acetylsalicylate (Table 5), suggesting that esterase activity of the protein preparation indeed is a property of *N*-acetylanthranilate amidase rather than a contaminating esterase. Analogous results were obtained for His_6Amq (data not shown).

Secondary structure estimates from CD spectra. CD spectra of His_6Amq and His_6AmqC22A/C63A show some differences, especially in the wavelength range between 205 and 225 nm. The cysteine-deficient protein shows a significant minimum at 208 nm, which is characteristic for α-helical proteins and does

TABLE 5. Specific activities and enrichment factors of His_6AmqC22A/C63A during purification, measured with *N*-acetylanthranilate (amide) and acetylsalicylate (ester)

Purification step	Sp act (U/mg)		Purification (*x*-fold)	
	Amide	Ester	Amide	Ester
Crude extract	0.6	0.6	1	1
Ni sepharose	69	56	115	93
AEX[a]	160	124	267	207

[a] AEX, anion exchange chromatography.

TABLE 6. Deconvolution of the CD spectra by the CDNN software of Böhm et al. (11)[a]

Secondary structural motif	His_6Amq	His_6AmqC22A/C63A
α-Helix	40.8	54.7
Antiparallel β-sheet	9.3	5.2
Parallel β-sheet	5.6	5.4
β-Turn	16.0	13.5
Aperiodic structure	28.3	22.7
Total sum	100.0	101.4

[a] The wavelength range taken into account was 210 to 260 nm. The numbers give the percentage of the respective secondary structural motif.

not appear in the His_6Amq protein. Furthermore, the typical α-helical minimum at 222 nm, which both proteins show, is more pronounced in the protein carrying the cysteine-to-alanine replacements than in His_6Amq. These findings suggest the occurrence of a higher α-helical content in His_6AmqC22A/C63A than in the tagged wild-type protein.

Deconvolution of the spectra using the program K2D by Andrade et al. (8) results in the same amounts of α-helices and β-sheet for either type of the protein; the values are 37% α-helix, 26% β-sheet, and 38% aperiodic structures. The results obtained with the more sophisticated software of Böhm et al. (11) are summarized in Table 6. The parameters between 210 and 260 nm are probably most reliable due to highest experimental accuracy in that wavelength range, so only these values were taken into account for the deconvolution. The result of the deconvolution clearly shows that the α-helical content increases with the cysteine-to-alanine exchanges in positions 22 and 63 at the expense of β-sheets and aperiodic structures. Both deconvolution programs unambiguously indicate α/β-folding motifs. The CDNN program uses as its basis a set of 33 spectra of known secondary structures, whereas the K2D program uses only 15. Because of this broader basis of reference sets, we consider the results of the CDNN software more reliable. Its application supports quantitatively the nonidentity of the CD spectra shown in Fig. 5. The most pronounced difference is evidently a higher degree of α-helicity in the cysteine-deficient protein variant.

DISCUSSION

Aryl-acylamidases occur in both eukaryotic organisms (22, 36, 43) and prokaryotes (3, 18, 26, 30, 31, 37, 42). Whereas aryl-acylamidase activity in vertebrates usually (but not invariably) is associated with cholinesterases (14, 23), which belong to the α/β-hydrolase-fold superfamily of proteins, the assignment of most bacterial aryl-acylamidases to enzyme families is not known due to lack of sequence information. An exception is carbamate hydrolase from *Arthrobacter oxydans* P52, a 55-kDa protein with minor amidase activity, which indeed shows significant similarity to eukaryotic acetylcholinesterase and other large carboxylesterases (55). However, Amq from *A. nitroguajacolicus* Rü61a, in contrast to cholinesterases, is a small protein, with only a few insertions and extensions in the presumed α/β-hydrolase core fold. Rather, it belongs to the esterase/lipase/thioesterase family (IPR000379) within the α/β-hydrolase fold superfamily.

Most of the studies on bacterial aryl-acylamidases were focused on the catabolism of acetanilide and phenylcarbamate pesticides. Amq, which was produced as a His_6-tagged protein in *E. coli*, is able to catalyze hydrolysis of the acylanilide herbicide propanil (3′,4′-dichloroacetanilide) with a low level of activity, but the more complex acylanilide herbicide propachlor and the carbamate herbicides tested were not hydrolyzed. The inability of *A. nitroguajacolicus* Rü61a to utilize or cometabolically convert propanil, and the localization of the *amq* gene within a gene cluster coding for the enzymes of quinaldine conversion to anthranilate (52), suggest that *amq* has evolved to take part in this specific catabolic pathway rather than in herbicide detoxification. However, its esterase activity might confer an additional physiological function.

In comparing the activity of Amq towards acetanilides, it is remarkable that Amq appeared to be inactive towards *m*- and *p*-nitroacetanilide, whereas *o*-nitroacetanilide, which exerts a similar electron-withdrawing effect, was hydrolyzed. In its preference towards *o*-nitroacetanilide, Amq functionally resembles human acetylcholinesterase rather than aryl-acylamidase from *P. fluorescens*, which hydrolyzes *p*-nitroacetanilide with higher levels of activity than the *o*-nitro analogue (14). ^{1}H-nuclear magnetic resonance analyses performed by Darvesh et al. (14) suggested that *o*-nitroacetanilide forms a six-membered cyclic species involving intramolecular hydrogen bonding between the oxygen of the nitro substituent and the amide hydrogen. *N*-acetylanthranilate, the physiological substrate of Amq, may form an analogous intramolecular hydrogen bond (Fig. 6). The hypothesis that intramolecular hydrogen bonding facilitates hydrolysis of the amide bond by Amq is consistent with its low level of activity towards acetanilide and apparent inactivity towards *o*-aminoacetanilide. However, substrate specificities reported for other bacterial aryl-acylamidases indicate that preference for *ortho*-substituted anilides which can form such hydrogen-bonded species is not a general feature of these

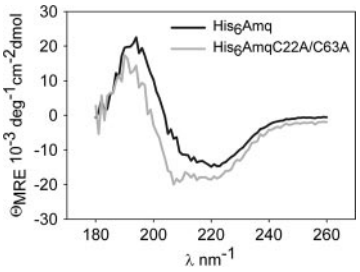

FIG. 5. CD spectra of His_6Amq and His_6AmqC22A/C63A. The spectra were recorded in a 0.1-mm cuvette. deg, degree.

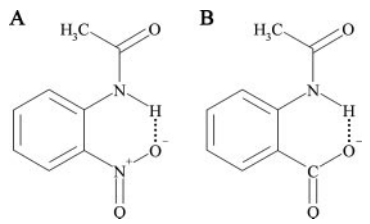

FIG. 6. Presumed hydrogen bonding in *o*-nitroacetanilide (A) and *N*-acetylanthranilate (B).

enzymes. Aryl-acylamidase from *P. acidovorans* AE1 actually hydrolyzes acetanilide, *p*-nitroacetanilide, and *o*-nitroacetanilide with similar activity (6); the activity of aryl-acylamidase from *Nocardia globerula* IFO 13510 towards acetanilide and *p*-nitroacetanilide also is similar, but this enzyme barely converts *o*-nitroacetanilide, presumably due to steric hindrance of *ortho* substituents (70). The amino acid sequences of the amidases from *P. acidovorans* (a 57-kDa monomer) and *N. globerula* (a 126-kDa homodimer) are not known.

Hydrolysis of ester bonds by Amq clearly follows other rules than cleavage of the amide bond. Among the substrates tested, phenylacetate was converted best, suggesting that the ester bond is destabilized more easily than the corresponding amide bond and confirming that a polar or acidic *ortho* substituent at the aromatic ring is not per se beneficial for Amq-catalyzed hydrolytic reactions. The *ortho*-carboxy group (in acetylsalicylate) even adversely affected ester hydrolysis by Amq. Activity towards aryl-acylesters has been reported for other aryl-acylamidases; however, the specificities again are different for enzymes from different sources. Activity of the *Nocardia* enzyme, for example, towards phenylacetate is about 76% of its activity towards the amide analogue, acetanilide (70). Aryl-acylamidase from strain AE1 converts *p*-nitrophenylacetate with higher levels of activity than phenylacetate; its catalytic efficiency with phenylacetate and acetanilide is very similar (6).

The activity of the protein variant His_6AmqC22A/C63A towards some, but not all, substrates tested was significantly greater than the activity of His_6Amq. Even if PAGE analysis of His_6Amq kept in the BR buffer of the standard assay (in contrast to protein in Tris buffer) did not reveal additional bands due to intra- and intermolecular disulfide bond formation, some general increase in activity of His_6AmqC22A/C63A versus His_6Amq might be due to the fact that the cysteineless protein is stable in its single monomeric form. However, such general effects cannot account for drastic and/or differential changes in apparent k_{cat} and the effects of the substitutions on apparent K_ms. As indicated by the CD spectra of His_6Amq and His_6AmqC22A/C63A, the cysteine replacements resulted in a significant change of the overall fold of the protein. We assume that these overall changes in conformation are also pertinent to the structure of the active site of the enzyme. If so, they could account for the observed drastic decrease in the apparent k_{cat} for the conversion of the formyl amide *N*-formylanthranilate, the increases in k_{cat} of the enzyme for most aryl-acetylamides and -esters, and the changes in K_ms. However, an in-depth explanation for the kinetic behavior of His_6AmqC22A/C63A versus His_6Amq is not possible in the absence of additional spectroscopic, calorimetric, and structural data.

ACKNOWLEDGMENTS

We thank Wiebke Frank for initial construction of pWFAAM and Alexander Albers for construction of His_6AmqC22A/C63A. We are grateful to A. Steinbüchel and M. Obst (WWU Münster) for kindly providing cyanophycin and for HPLC analysis of cyanophycin assays.

REFERENCES

1. **Aboulmagd, E., F. B. Oppermann-Sanio, and A. Steinbüchel.** 2000. Molecular characterization of the cyanophycin synthetase from *Synechocystis* sp. strain PCC6308. Arch. Microbiol. **174:**297–306.
2. **Aiyar, A.** 2000. The use of CLUSTAL W and CLUSTAL X for multiple sequence alignment. Methods Mol. Biol. **132:**221–241.
3. **Akutsu-Shigeno, Y., Y. Adachi, C. Yamada, K. Toyoshima, N. Nomura, H. Uchiyama, and T. Nakajima-Kambe.** 2006. Isolation of a bacterium that degrades urethane compounds and characterization of its urethane hydrolase. Appl. Microbiol. Biotechnol. **70:**422–429.
4. **Alam, M., D. E. Vance, and R. Lehner.** 2002. Structure-function analysis of human triacylglycerol hydrolase by site-directed mutagenesis: identification of the catalytic triad and a glycosylation site. Biochemistry **41:**6679–6687.
5. **Allebrandt, K. V., V. Rajesh, and P. G. Layer.** 2005. Expression of acetylcholinesterase (AChE) and aryl acylamidase (AAA) during early zebrafish embryogenesis. Chem. Biol. Interact. **157–158:**353–355.
6. **Alt, J., E. Heymann, and K. Krisch.** 1975. Characterization of an inducible amidase from *Pseudomonas acidovorans* AE1. Eur. J. Biochem. **53:**357–369.
7. **Altschul, S. F., T. L. Madden, A. A. Schäffer, J. Zhang, Z. Zhang, W. Miller, and D. J. Lipman.** 1997. Gapped BLAST and PSI-BLAST: a new generation of protein database search programs. Nucleic Acids Res. **25:**3389–3402.
8. **Andrade, M. A., P. Chacon, J. J. Merelo, and F. Moran.** 1993. Evaluation of secondary structure of proteins from UV circular dichroism spectra using an unsupervised learning neural network. Protein Eng. **6:**383–390.
9. **Arand, M., F. Müller, A. Mecky, W. Hinz, P. Urban, D. Pompon, R. Kellner, and F. Oesch.** 1999. Catalytic triad of microsomal epoxide hydrolase: replacement of Glu404 with Asp leads to a strongly increased turnover rate. Biochem. J. **337:**37–43.
10. **Barth, S., M. Fischer, R. D. Schmid, and J. Pleiss.** 2004. Sequence and structure of epoxide hydrolases: a systematic analysis. Proteins **55:**846–855.
11. **Böhm, G., R. Muhr, and R. Jaenicke.** 1992. Quantitative analysis of protein far UV circular dichroism spectra by neural networks. Protein Eng. **5:**191–195.
12. **Boopathy, R., and P. G. Layer.** 2004. Aryl acylamidase activity on acetylcholinesterase is high during early chicken brain development. Protein J. **23:**325–333.
13. **Chavira, R., T. J. Burnett, and J. H. Hageman.** 1984. Assaying proteinases with azocoll. Anal. Biochem. **136:**446–450.
14. **Darvesh, S., R. S. McDonald, K. V. Darvesh, D. Mataija, S. Mothana, H. Cook, K. M. Carneiro, N. Richard, R. Walsh, and E. Martin.** 2006. On the active site for hydrolysis of aryl amides and choline esters by human cholinesterases. Bioorg. Med. Chem. **14:**4586–4599.
15. **Da Silva, A. C. R., J. A. Ferro, F. C. Reinach, C. S. Farah, L. R. Furlan, R. Quaggio, C. B. Monteiro-Vitorello, M. A. Van Sluys, N. F. Almeida, L. M. C. Alves, A. M. do Amaral, M. C. Bertolini, L. E. A. Camargo, G. Camarotte, F. Cannavan, J. Cardozo, F. Chambergo, L. P. Ciapina, R. M. Cicarelli, L. L. Coutinho, J. R. Cursino-Santos, H. El-Dorry, J. B. Faria, A. J. Ferreira, R. C. Ferriera, M. I. Ferro, E. F. Formichieri, M. C. Franco, C. C. Greggio, A. Gruber, A. M. Katsuyama, L. T. Kishi, R. P. Leite, E. G. Lemos, M. V. Lemos, E. C. Locali, M. A. Machado, A. M. Madeira, N. M. Martinez-Rossi, E. C. Martins, J. Meidanis, C. F. Menck, C. Y. Miyaki, D. H. Moon, L. M. Moreira, M. T. Novo, V. K. Okura, M. C. Oliveira, V. R. Oliveira, H. A. Pereira, A. Rossi, J. A. Sena, C. Silva, R. F. de Souza, L. A. Spinola, M. A. Takita, R. E. Tamura, E. C. Teixeira, R. I. Tezza, M. Trindade dos Santos, D. Truffi, S. M. Tsai, F. F. White, J. C. Setubal, and J. P. Kitajima.** 2002. Comparison of the genomes of two *Xanthomonas* pathogens with differing host specificities. Nature **417:**459–463.
16. **Dembek, G., T. Rommel, F. Lingens, and H. Höke.** 1989. Degradation of quinaldine by *Alcaligenes* sp. and by *Arthrobacter* sp. FEBS Lett. **246:**113–116.
17. **Diaz, E., and K. N. Timmis.** 1995. Identification of functional residues in a 2-hydroxymuconic semialdehyde hydrolase. A new member of the alpha/beta hydrolase-fold family of enzymes which cleaves carbon-carbon bonds. J. Biol. Chem. **270:**6403–6411.
18. **Engelhardt, G., P. R. Wallnöfer, and R. Plapp.** 1973. Purification and properties of an aryl acylamidase of *Bacillus sphaericus*, catalyzing the hydrolysis of various phenylamide herbicides and fungicides. Appl. Microbiol. **26:**709–718.
19. **Fetzner, S.** 1998. Bacterial degradation of pyridine, indole, quinoline, and their derivatives under different redox conditions. Appl. Microbiol. Biotechnol. **49:**237–250.
20. **Frerichs-Deeken, U., K. Ranguelova, R. Kappl, J. Hüttermann, and S. Fetzner.** 2004. Dioxygenases without requirement for cofactors and their model reaction: compulsory order ternary complex mechanism of 1*H*-3-hydroxy-4-oxoquinaldine 2,4-dioxygenase involving general base catalysis by histidine 251 and single-electron oxidation of the substrate dianion. Biochemistry **43:**14485–14499.
21. **Frerichs-Deeken, U., and S. Fetzner.** 2005. Dioxygenases without requirement for cofactors: identification of amino acid residues involved in substrate binding and catalysis, and testing for rate-limiting steps in the reaction of 1*H*-3-hydroxy-4-oxoquinaldine 2,4-dioxygenase. Curr. Microbiol. **51:**344–352.
22. **Fukuda, K., T. Matsumoto, K. Hagiwara, Z. Fujimoto, and H. Mizuno.** 1997. Crystallization and preliminary X-ray diffraction studies of tulip aryl acylamidase: a key enzyme in plant herbicide detoxification. Acta Crystallogr. D **53:**342–344.
23. **George, S. T., and A. S. Balasubramanian.** 1981. The aryl acylamidases and their relationship to cholinesterases in human serum, erythrocyte and liver. Eur. J. Biochem. **121:**177–186.

24. **Gibney, G., S. Camp, M. Dionne, K. MacPhee-Quigley, and P. Taylor.** 1990. Mutagenesis of essential functional residues in acetylcholinesterase. Proc. Natl. Acad. Sci. USA **87:**7546–7550.
25. **Grant, S. G. N., J. Jessee, F. R. Bloom, and D. Hanahan.** 1990. Differential plasmid rescue from transgenic mouse DNAs into *Escherichia coli* methylation-restriction mutants. Proc. Natl. Acad. Sci. USA **87:**4645–4649.
26. **Hammond, P. M., C. P. Price, and M. D. Scawen.** 1983. Purification and properties of aryl acylamidase from *Pseudomonas fluorescens* ATCC 39004. Eur. J. Biochem. **132:**651–655.
27. **Hanahan, D.** 1983. Studies on transformation of *Escherichia coli* with plasmids. J. Mol. Biol. **166:**557–580.
28. **Hanes, C. S.** 1932. Studies on plant amylases. I. The effect of starch concentration upon the velocity of hydrolysis by the amylase of germinated barley. Biochem. J. **26:**1406–1421.
29. **Heikinheimo, P., A. Goldman, C. Jeffries, and D. L. Ollis.** 1999. Of barn owls and bankers: a lush variety of alpha/beta hydrolases. Structure **7:**R141–R146.
30. **Heymann, E., and H. Rix.** 1978. The active site of an inducible arylacylamidase from *Pseudomonas acidovorans*. Int. J. Pept. Protein Res. **11:**59–64.
31. **Hirase, K., and S. Matsunaka.** 1991. Purification and properties of propanil hydrolase in *Pseudomonas pickettii*. Pest. Biochem. Physiol. **39:**302–308.
32. **Holloway, P., J. T. Trevors, and H. Lee.** 1998. A colorimetric assay for detecting haloalkane dehalogenase activity. J. Microbiol. Methods **32:**31–36.
33. **Hooft, R. W. W., G. Vriend, C. Sander, and E. E. Abola.** 1996. Errors in protein structures. Nature **381:**272.
34. **Hund, H. K., A. de Beyer, and F. Lingens.** 1990. Microbial metabolism of quinoline and related compounds. VI. Degradation of quinaldine by *Arthrobacter* sp. Biol. Chem. Hoppe-Seyler **371:**1005–1008.
35. **Hynkova, K., Y. Nagata, M. Takagi, and J. Damborsky.** 1999. Identification of the catalytic triad in the haloalkane dehalogenase from *Sphingomonas paucimobilis* UT26. FEBS Lett. **446:**177–181.
36. **Jun, C. J., and S. Matsunaka.** 1990. The propanil hydrolyzing enzyme aryl acylamidase in the wild rices of genus *Oryza*. Pest. Biochem. Physiol. **38:** 26–33.
37. **Kearney, P. C.** 1965. Purification and properties of an enzyme responsible for hydrolyzing phenylcarbamates. J. Agric. Food Chem. **13:**561–564.
38. **Laane, C., S. Boeren, K. Vos, and C. Veeger.** 1987. Rules for optimization of biocatalysis in organic solvents. Biotechnol. Bioeng. **30:**81–87.
39. **Laemmli, U. K.** 1970. Cleavage of structural proteins during the assembly of the head of bacteriophage T4. Nature **227:**680–685.
40. **Li, C., M. G. Montgomery, F. Mohammed, J. J. Li, S. P. Wood, and T. D. Bugg.** 2005. Catalytic mechanism of C-C hydrolase MhpC from *Escherichia coli*: kinetic analysis of His263 and Ser110 site-directed mutants. J. Mol. Biol. **346:**241–251.
41. **Marchler-Bauer, A., and S. H. Bryant.** 2004. CD-Search: protein domain annotations on the fly. Nucleic Acids Res. **32:**W327–W331.
42. **Marty, J. L., and J. Vouges.** 1987. Purification and properties of a phenylcarbamate herbicide degrading enzyme of *Pseudomonas alcaligenes* isolated from soil. Agric. Biol. Chem. **51:**3287–3294.
43. **Matsunaka, S.** 1968. Propanil hydrolysis: inhibition in rice plants by insecticides. Science **160:**1360–1361.
44. **Morel, F., C. Gilbert, C. Geourjon, J. Frot-Coutaz, R. Portalier, and D. Atlan.** 1999. The prolyl aminopeptidase from *Lactobacillus delbrueckii* subsp. bulgaricus belongs to the alpha/beta hydrolase fold family. Biochim. Biophys. Acta **1429:**501–505.
45. **Nardini, M., and B. W. Dijkstra.** 1999. Alpha/beta hydrolase fold enzymes: the family keeps growing. Curr. Opin. Struct. Biol. **9:**732–737.
46. **National Center for Biotechnology Information Microbial Genomes Annotation Project.** 2004. *Ralstonia eutropha* JMP134. National Center for Biotechnology Information, National Institutes of Health, Bethesda, Md.
47. **Ollis, D. L., E. Cheah, M. Cygler, B. Dijkstra, F. Frolow, S. M. Franken, M. Harel, S. J. Remington, I. Silman, J. Schrag, J. L. Sussman, K. H. G. Verschuren, and A. Goldman.** 1992. The alpha/beta hydrolase fold. Protein Eng. **5:**197–211.
48. **Ordentlich, A., D. Barak, C. Kronman, N. Ariel, Y. Segall, B. Velan, and A. Shafferman.** 1998. Functional characteristics of the oxyanion hole in human acetylcholinesterase. J. Biol. Chem. **273:**19509–19517.
49. **Overhage, J., S. Sielker, S. Homburg, K. Parschat, and S. Fetzner.** 2005. Identification of large linear plasmids in *Arthrobacter* spp. coding for the degradation of quinaldine to anthranilate. Microbiology **151:**491–500.
50. **Pabarcus, M. K., and J. E. Casida.** 2002. Kynurenine formamidase: determination of primary structure and modeling-based prediction of tertiary structure and catalytic triad. Biochim. Biophys. Acta **1596:**201–211.
51. **Pace, C. N., F. Vajdos, L. Fee, G. Grimsley, and T. Gray.** 1995. How to measure and predict the molar absorption coefficient of a protein. Protein Sci. **4:**2411–2423.
52. **Parschat, K., B. Hauer, R. Kappl, R. Kraft, J. Hüttermann, and S. Fetzner.** 2003. Gene cluster of *Arthrobacter ilicis* Rü61a involved in the degradation of quinaldine to anthranilate. Characterization and functional expression of the quinaldine 4-oxidase *qoxLMS* genes. J. Biol. Chem. **278:**27483–27494.
53. **Pelletier, I., J. Altenbuchner, and R. Mattes.** 1995. A catalytic triad is required by the non-heme haloperoxidases to perform halogenation. Biochim. Biophys. Acta **1250:**149–157.
54. **Pleiss, J., M. Fischer, M. Peiker, C. Thiele, and R. D. Schmid.** 2000. Lipase engineering database: understanding and exploiting sequence–structure–function relationships. J. Mol. Catal. B. **10:**491–508.
55. **Pohlenz, H.-D., W. Boidol, I. Schüttke, and W. R. Streber.** 1992. Purification and properties of an *Arthrobacter oxydans* P52 carbamate hydrolase specific for the herbicide phenmedipham and nucleotide sequence of the corresponding gene. J. Bacteriol. **174:**6600–6607.
56. **Pries, F., J. Kingma, G. H. Krooshof, C. M. Jeronimus-Stratingh, A. P. Bruins, and D. B. Janssen.** 1995. Histidine 289 is essential for hydrolysis of the alkyl-enzyme intermediate of haloalkane dehalogenase. J. Biol. Chem. **270:**10405–10411.
57. **Rainey, F. A., N. Ward-Rainey, R. M. Kroppenstedt, and E. Stackebrandt.** 1996. The genus *Nocardiopsis* represents a phylogenetically coherent taxon and a distinct actinomycete lineage: proposal of *Nocardiopsaceae* fam. nov. Int. J. Syst. Bacteriol. **46:**1088–1092.
58. **Rauen, H. M.** 1964. Biochemisches Taschenbuch; Zweiter Teil. Springer-Verlag, Heidelberg, Germany.
59. **Rink, R., M. Fennema, M. Smids, U. Dehmel, and D. B. Janssen.** 1997. Primary structure and catalytic mechanism of the epoxide hydrolase from *Agrobacterium radiobacter* AD1. J. Biol. Chem. **272:**14650–14657.
60. **Rost, B., G. Yachdav, and J. Liu.** 2004. The PredictProtein server. Nucleic Acids Res. **32:**W321–W326.
61. **Rost, B., and C. Sander.** 1993. Prediction of protein secondary structure at better than 70% accuracy. J. Mol. Biol. **232:**584–599.
62. **Sambrook, J., E. Fritsch, and T. Maniatis.** 1989. Molecular cloning: a laboratory manual, 2nd ed. Cold Spring Harbor Laboratory Press, Cold Spring Harbor, N.Y.
63. **Sambrook, J., and D. W. Russell.** 2001. Molecular cloning: a laboratory manual, 3rd ed. Cold Spring Harbor Laboratory Press, Cold Spring Harbor, N.Y.
64. **Schwede, T., J. Kopp, N. Guex, and M. C. Peitsch.** 2003. SWISS-MODEL: an automated protein homology-modeling server. Nucleic Acids Res. **31:**3381–3385.
65. **Tai, M. H., S. S. Chirala, and S. J. Wakil.** 1993. Roles of Ser101, Asp236, and His237 in catalysis of thioesterase II and of the C-terminal region of the enzyme in its interaction with fatty acid synthase. Proc. Natl. Acad. Sci. USA **90:**1852–1856.
66. **Taylor, P., and Z. Radic.** 1994. The cholinesterases: from genes to proteins. Annu. Rev. Pharmacol. Toxicol. **34:**281–320.
67. **Towbin, H., T. Staehelin, and J. Gordon.** 1979. Electrophoretic transfer of proteins from polyacrylamide gels to nitrocellulose sheets: procedure and some applications. Proc. Natl. Acad. Sci. USA **76:**4350–4354.
68. **Vaughan, P. A., G. F. Hall, and D. J. Best.** 1990. Aryl acylamidase from *Rhodococcus erythropolis* NCIB 12273. Appl. Microbiol. Biotechnol. **34:** 42–46.
69. **Weatherburn, M. W.** 1967. Phenol-hypochlorite reaction for determination of ammonia. Anal. Chem. **39:**971–974.
70. **Yoshioka, H., T. Nagasawa, and H. Yamada.** 1991. Purification and characterization of aryl acylamidase from *Nocardia globerula*. Eur. J. Biochem. **199:**17–24.
71. **Zock, J., C. Cantwell, J. Swartling, R. Hodges, T. Pohl, K. Sutton, P. Rosteck, Jr., D. McGilvray, and S. Queener.** 1994. The *Bacillus subtilis pnbA* gene encoding *p*-nitrobenzyl esterase: cloning, sequence and high-level expression in *Escherichia coli*. Gene **151:**37–43.
72. **Zor, T., and Z. Selinger.** 1996. Linearization of the Bradford protein assay increases its sensitivity: theoretical and experimental studies. Anal. Biochem. **236:**302–308.

JOURNAL OF BACTERIOLOGY, May 2007, p. 3933 Vol. 189, No. 10
0021-9193/07/$08.00+0 doi:10.1128/JB.00325-07

ERRATUM

N-Acetylanthranilate Amidase from *Arthrobacter nitroguajacolicus* Rü61a, an α/β-Hydrolase-Fold Protein Active towards Aryl-Acylamides and -Esters, and Properties of Its Cysteine-Deficient Variant

Stephan Kolkenbrock, Katja Parschat, Bernd Beermann, Hans-Jürgen Hinz, and Susanne Fetzner

Institut für Molekulare Mikrobiologie und Biotechnologie, and Institut für Physikalische Chemie, Westfälische Wilhelms-Universität Münster, D-48149 Münster, Germany

Volume 188, no. 24, p. 8430–8440, 2006. Page 8431, Fig. 1: As the compound released from *N*-acetylanthranilate in the reaction catalyzed by *N*-acetylanthranilate amidase (IV) is acetate, the pathway shown should appear as shown below.